Airborne Visible/Infrared Imaging Spectrometer (AVIRIS)

Spectrometer Design and Performance

by

Steven A. Macenka
Michael P. Chrisp, Ph.D.

Jet Propulsion Laboratory
California Institute of Technology
Pasadena, California

ABSTRACT

The development of the Airborne Visible/Infrared Imaging Spectrometer (AVIRIS) has been completed at the Jet Propulsion Laboratory, California Institute of Technology. This paper outlines the functional requirements for the spectrometer optics subsystem, and describes the spectrometer optical design. The optical subsystem performance is shown in terms of spectral modulation transfer functions, radial energy distributions and system transmission at selected wavelengths for the four spectrometers. An outline of the spectrometer alignment is included.

1. INTRODUCTION

The Airborne Visible/Infrared Imaging Spectrometer has been developed at the Jet Propulsion Laboratory as a NASA facility instrument to fly on a U2 aircraft. Its purpose is to provide high quality spectral data for remote sensing. The science requirements that had to be met to achieve this are given in Table 1. The spectral range extending from 0.4 μm to 2.4 μm was divided into four parts to provide a uniform signal-to-noise ratio over the whole spectral range. This division was required to maintain the diffraction grating efficiency over the given spectral ranges. One of the prime objectives of the instrument was mineral identification from spectral signatures. To do this, the spectral sampling interval was chosen based on the requirement to resolve the kaolinite doublet at 2.2 μm wavelength, shown in Fig. 1. The intensity modulation of this spectral feature is ≤ 0.05 at a spectral frequency of 0.04 cycles/nanometer (c/nm), or, in terms of spatial frequency in the detector plane, it is 2.0 c/mm. To resolve this doublet required that the modulation transfer function MTF $\geq$ 0.5 at 2.0 c/mm for the AVIRIS spectrometers. This optical performance guarantees the resolution of the kaolinite doublet and provides an acceptable instrument spectral responsivity function, illustrated for a Gaussian point spread function in Fig. 2.

Table 1. AVIRIS Science Requirements

Spectral Coverage	0.4 to 2.4 μm	Swath Width (from U2)	$\geq$ 10 km
Spectral Sampling Interval	$\leq$ 10 nm	Spatial Oversample	$\geq$ 15%
Signal-to-noise Ratio	$\geq$ 100:1 at 0.7 μm	Calibration	
	$\geq$ 50:1 at 2.2 μm	Relative	0.5%
Instantaneous Field of View (IFOV)	$\leq$ 1 mrad	Absolute	5% to 10%

The AVIRIS optics subsystem consists of a whiskbroom scanner connected by optical fibers to four spectrometers, shown schematically in Fig. 3. As the prismatic scan mirror rotates, the field-of-view is swept across the flight path. In the spectrometers the dispersed spectrum is imaged on cooled linear arrays of silicon detectors for the 0.4 μm to 0.7 μm spectral range and on indium antimonide arrays for the 0.7 μm to 2.45 μm spectral range. An onboard reference source is also connected by optical fibers to the spectrometers, providing information on spectral and radiometric calibration.

2. SPECTROMETER OPTICAL DESIGN

An all-reflective decentered aperture Schmidt design was selected for the AVIRIS spectrometers. The optical schematics of the AVIRIS spectrometers are shown in Fig. 4.

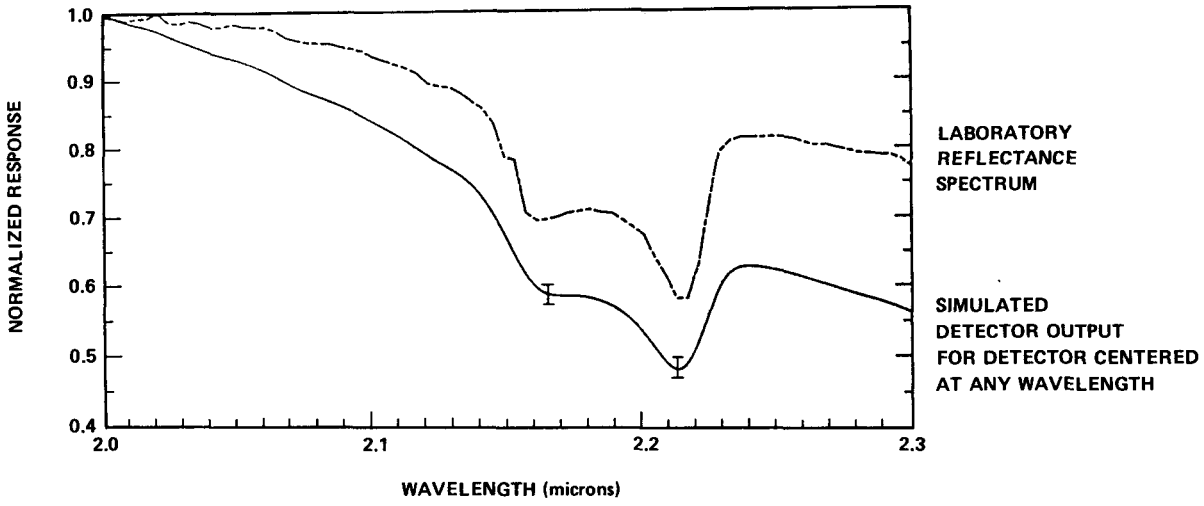

Fig. 1. Kaolinite Doublet Detection

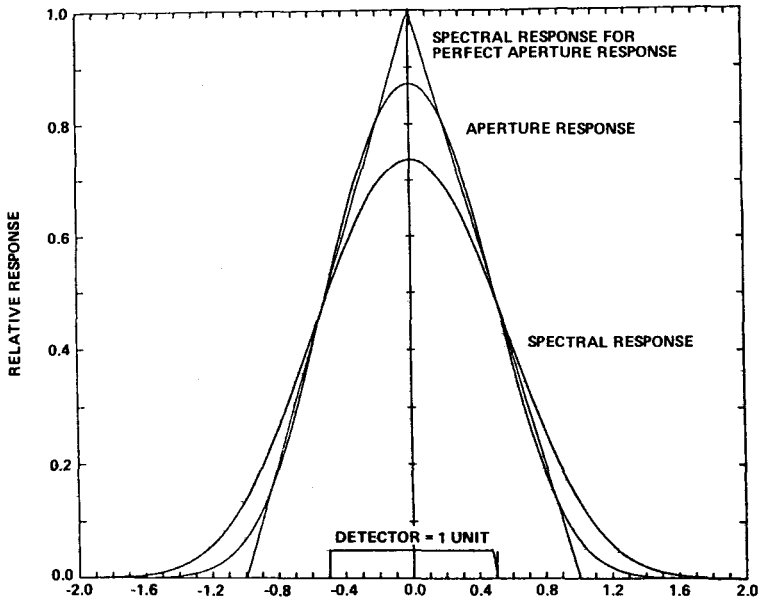

Fig. 2. Aperture Slit Detector Size

The radiant energy emerging from the fiber optic is collimated by a spherical mirror, which is used in double pass in this particular configuration. The reflective diffraction grating is located on the decentered aperture Schmidt corrector at the center of curvature of the collimating mirror. The grating mask forms the aperture stop of the spectrometer. All four AVIRIS spectrometers have the same basic optical layout and only the grating tilt changes significantly from Spectrometers "A" to "D", as required by the spectral range covered by each of the spectrometers. In this configuration, the Schmidt corrector plate is tilted with respect to the optical axis. The optimum surface figure for this particular configuration is an anamorphic aspheric surface. At the time of the AVIRIS implementation, the fabrication of such a surface was too risky and prohibitively expensive, so rotationally symmetric aspheric surfaces were selected for the AVIRIS spectrometer designs. This compromise resulted in a slight degradation of the overall optical performance but still stayed within the system specifications.

The AVIRIS spectrometer optical parameters are listed in Table 2. Shown in this table are the aspheric coefficients of the grating. The grating surface is given by the equation,

$$z = \frac{ch^2}{1 + \left[1 - (1+K)\, c^2h^2\right]^{1/2}} + Ah^4 + Bh^6 + Ch^8 + Dh^{10}$$

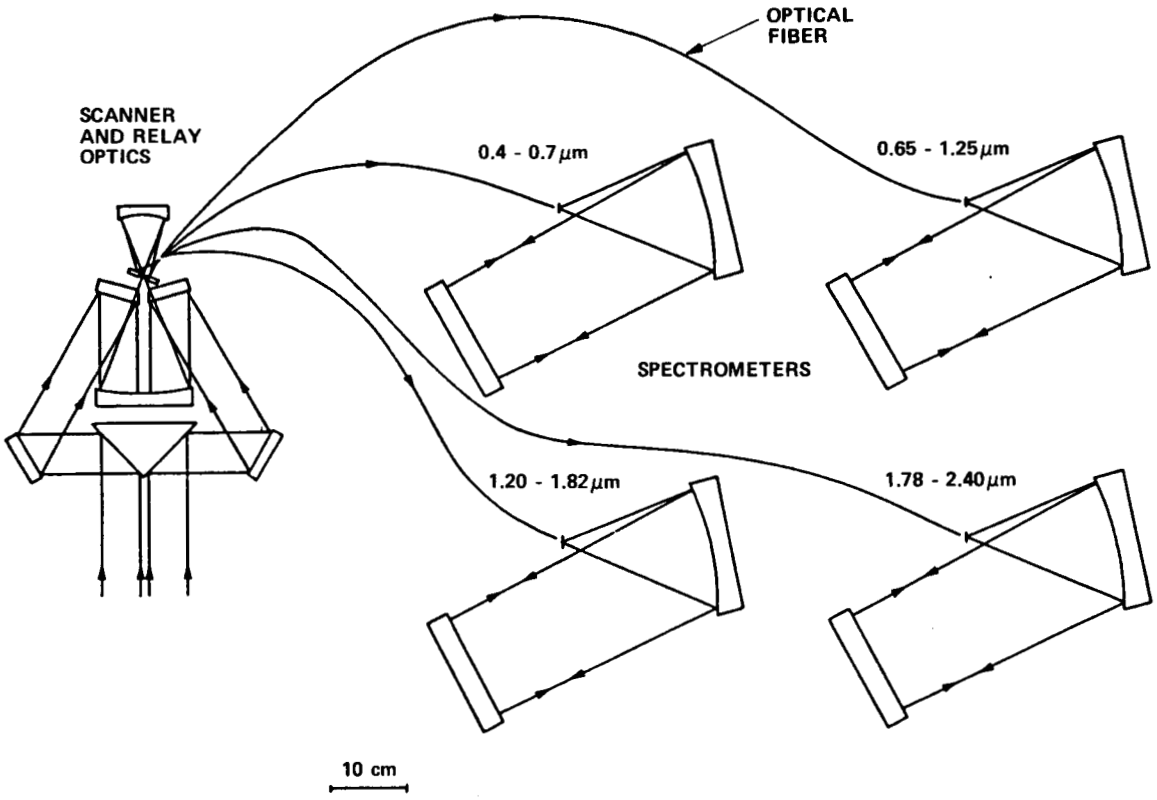

Fig. 3. AVIRIS Optics Schematic

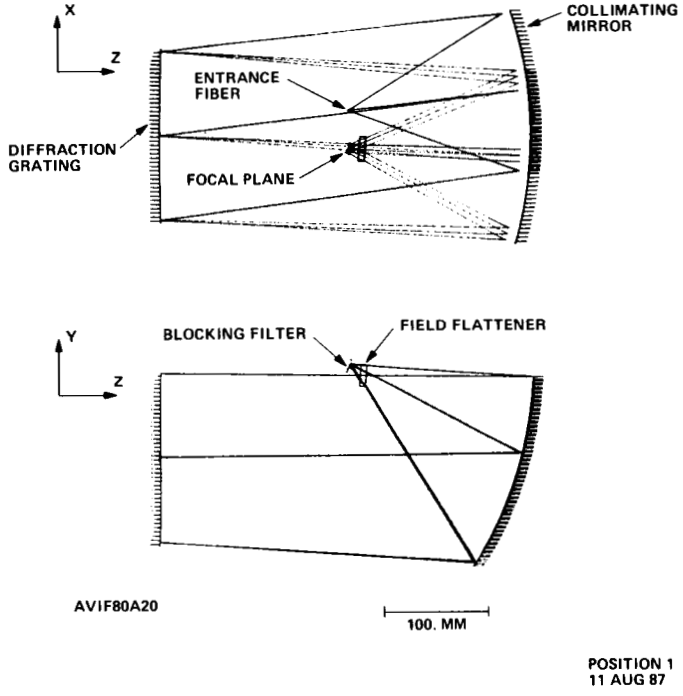

Fig. 4. AVIRIS "A" Spectrometer

In the table, α is the angle of incidence and ß is the angle of diffraction at the blaze wavelength. The blazed diffraction gratings were ruled on single-point diamond-turned aluminum substrates. The only refractive components in the spectrometers are the fused silica field flatteners and the blocking filters. The blocking filter specifications are summarized in Table 3, showing the required filter profiles.

Table 2. AVIRIS Spectrometer Optical Parameters

SPECTROMETER DESIGNATION	λ [nm]	COLLIM. R_2 [mm]	GRATING R_4 [mm]	ASPHERIC COEFFICIENTS A	B	C	D	CONIC CONSTANT	GROOVE SPACING [μm]	α [Deg]	β [Deg]
AVIF80A20	400 λ_B =550 750	379.50	2447.38	-3.0196E-9	-4.8493E-14	3.9799E-19	-1.7251E-23	-7.5968	8.5	7.07	3.35
AVIF80B20	650 λ_B =950 1250	374.41	3235.2	-3.3553E-9	-6.7655E-14	9.2947E-19	-2.8731E-23	-48.8671	7.80	8.83	1.84
AVIF80C20	1200 λ_B=1510 1820	370.51	3028.47	-3.3932E-9	-6.8325E-14	8.5751E-19	-2.5580E-23	-34.1756	8.05	10.70	0.16
AVIF75D20	1780 λ_B=2090 2400	359.75	2872.74	-3.4448E-9	-8.8769E-14	1.448E-18	-3.2394E-23	-52.0452	7.775	14.08	3.98

Table 3. AVIRIS Blocking Filter Specifications

FILTER NO.	SUGGESTED SUBSTRATE	SHORTWAVE STOPBAND λ_0	SHORTWAVE STOPBAND MAX. TRANS	PASSBAND λ_1	PASSBAND λ_2	LONGWAVE STOPBAND λ_3	LONGWAVE STOPBAND MAX TRANS
FILTER 1	SUPRASIL W1	0.35	1E-4	0.4	0.7	----	----
FILTER 2	SUPRASIL W1	0.625	1E-4	0.65	1.25	1.30	1E-4
FILTER 3	SUPRASIL W1	0.91	1E-4	1.20	1.82	2.50	1E-4
FILTER 4	SUPRASIL W1	1.20	1E-4	1.78	2.40	2.50	1E-4

ALL WAVELENGTHS IN μm

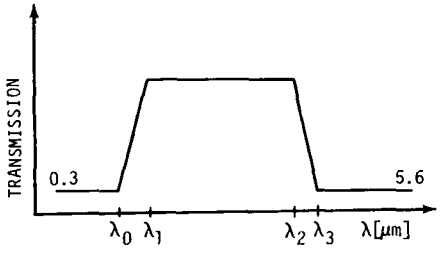

1. Operating Temp : T = 77°K
2. Adhesion of coatings per MIL-M-1308
3. Humidity per MIL-C-675A
4. Abrasion per MIL-C-675A
5. No pinholes within the clear aperture
6. In band transmittance shall be greater than 0.8 for all filters.
7. Transmission curves shall be supplied for all filters.
8. JPL Cog Engineer shall witness acceptance test.

The overall optical system transmittance is given in Tables 4 and 5. Most of the mirrors in the system for visible wavelengths have protected silver coatings. The relative diffraction efficiency measurements were made on plane sample gratings ruled with the same characteristics as the aspheric gratings.

The optical system theoretical performance has been analyzed in terms of spot diagrams (Fig. 5), with radial energy distributions shown in Figs. 6 and 7. Geometrical modulation transfer functions (MTF) and through focus MTF curves at the Nyquist frequency are given in Figs. 8, 9, 10, and 11. The system performance, including the detector MTFs, is given in Fig. 12, which shows that the MTF is greater than the 0.5 design goal at the 2.0 c/mm spatial frequency. Defining the effective spectral resolution for a sinusoidal distribution of radiance as the spectral half wavelength for which the modulation of the distribution of radiance has been reduced by one-half due to the MTF of the system, from Fig. 12, the resulting effective spectral resolution is approximately 10 nm.

Table 4. Transmittance of AVIRIS Optical System - Spectrometers A and B

		SPECTROMETER A				SPECTROMETER B			
		0.4	0.5	0.6	0.7	0.7	0.9	1.1	1.25
1	Hatch window (silica)	0.91	0.94	0.96	0.96	0.96	0.94	0.92	0.92
2	2 Reflections Al (Si0 coated)	$(0.86)^2$	$(0.88)^2$	$(0.88)^2$	$(0.87)^2$	$(0.87)^2$	$(0.90)^2$	$(0.95)^2$	$(0.96)^2$
3	7 Reflections Ag	$(0.82)^7$	$(0.98)^7$	$(0.98)^7$	$(0.98)^7$	$(0.98)^7$	$(0.98)^7$	$(0.98)^7$	$(0.98)^7$
4	Fiber Reflection Loss	0.88	0.88	0.88	0.88	0.88	0.88	0.88	0.88
5	NSG Fiber Transmittance	0.81	0.94	0.98	0.98	0.90	0.96	0.98	0.98
6	Relative Diffraction Efficiency	0.43	0.60	0.62	0.59	0.61	0.76	0.58	0.47
7	Window/Field Lens (silica)	0.91	0.91	0.91	0.91	0.91	0.91	0.91	0.91
8	Bandpass Filter	0.84	0.90	0.91	0.91	0.72	0.59	0.69	0.75
9	KDP Blocking Filter	N/A	N/A	N/A	N/A	0.93	0.93	0.93	0.93
	Total Transmittance	0.04	0.26	0.29	0.27	0.19	0.21	0.21	0.19

Note: The vignetting due to the light lost off the detector arrays (~30%) has not been included above.

Table 5. Transmittance of AVIRIS Optical System - Spectrometers C and D

		SPECTROMETER C				SPECTROMETER D				
		1.25	1.4	1.6	1.85	1.85	2.0	2.2	2.4	2.45
1	Hatch window (silica)	0.92	0.92	0.91	0.91	0.91	0.90	0.90	0.89	0.88
2	4 Reflections Al (Si0 coated)	$(0.96)^4$	$(0.96)^4$	$(0.97)^4$	$(0.97)^4$	$(0.97)^4$	$(0.97)^4$	$(0.97)^4$	$(0.97)^4$	$(0.97)^4$
3	5 Reflections Ag	$(0.98)^5$	$(0.98)^5$	$(0.98)^5$	$(0.98)^5$	$(0.98)^5$	$(0.98)^5$	$(0.98)^5$	$(0.98)^5$	$(0.98)^5$
4	Fiber Reflection Loss	0.89	0.89	0.89	0.89	0.89	0.89	0.89	0.89	0.89
5	Verre Fluore Fiber Transmittance	0.94	0.92	0.92	0.94	0.94	0.95	0.95	0.96	0.96
6	Relative Diffraction Efficiency	0.65	0.67	0.65	0.55	0.63	0.67	0.66	0.64	0.63
7	Window/Field Lens (silica)	0.91	0.91	0.91	0.91	0.91	0.91	0.91	0.91	0.91
8	Bandpass Filter	0.64	0.75	0.68	0.72	0.73	0.78	0.63	0.57	0.04
	Total Transmittance	0.22	0.26	0.24	0.22	0.26	0.29	0.23	0.20	0.01

Note: The vignetting due to the light lost off the detector arrays (~30%) has not been included above.

3. SPECTROMETER IMPLEMENTATION AND ALIGNMENT

The implementation of the spectrometer designs was challenging due to their high numerical aperture (N.A. = 0.45). To facilitate the alignment of the spectrometers the degrees of freedom were carefully chosen as shown in Fig. 13, enabling the line spectra to be focused and aligned on the arrays. To provide optimum light coupling from the optical fibers into the spectrometers, the fibers are mounted in the sphere arrangement shown in

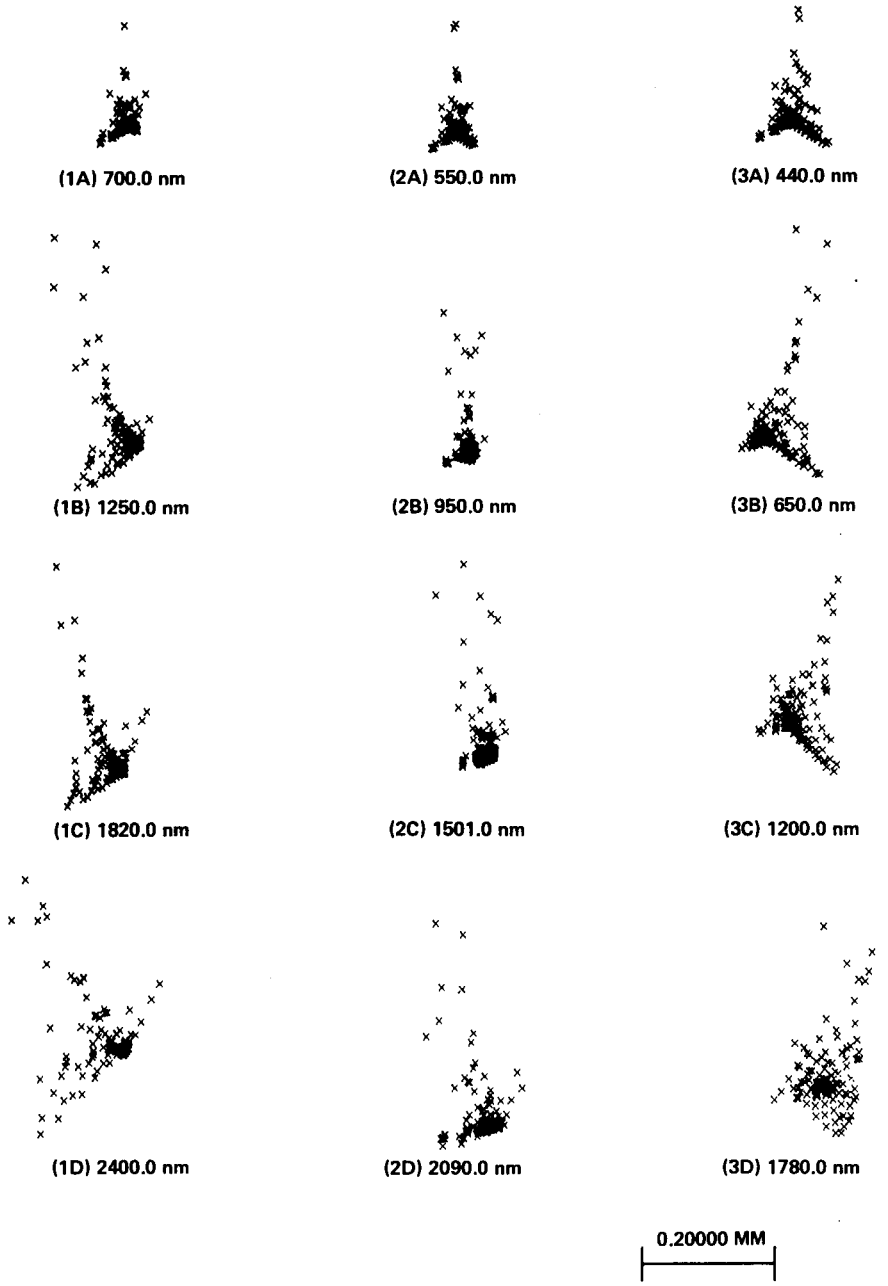

Fig. 5. AVIRIS Spectrometer Spot Diagram

Fig. 14. Rotation of the sphere allows the light from the central fiber (from the fore-optics) to be directed onto the collimating mirror without transverse displacement of the fiber. The grating mount design is shown in Fig. 15. This kinematic mount design allows the grating angle to be changed in two orthogonal directions to position the spectrum on the linear array. The grating is mounted kinematically in a cell to ensure minimal distortion. Spherical washer sets are used to ensure that no torquing forces are experienced by the cell as the shims are varied to change its angle. The mirror mount design is shown in Fig. 16, and again kinematic mount principles were followed to minimize the mirror distortion and provide ease of angular adjustment. The alignment of the spectrometers was accomplished by using higher diffracted orders of a HeNe laser at λ = 632.8 nm. First the higher orders were simulated by computer raytrace, which generated information about the position and image quality (point spread functions) in the spectrometer focal plane. This computer generated raytrace served as a baseline for evaluation of image quality and location in the focal plane during the actual alignment. The only remaining alignment was required for the detector assembly, which included the filters and the field flatteners. Focusing was accomplished by axial displacement of the optical fiber mount shown in Fig. 14.

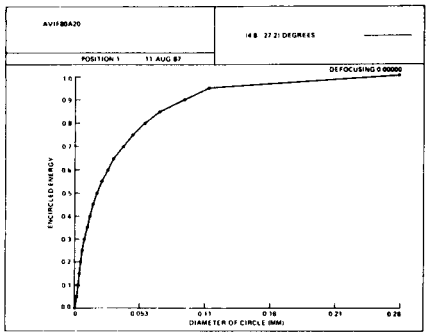

(1A) 700.0 nm

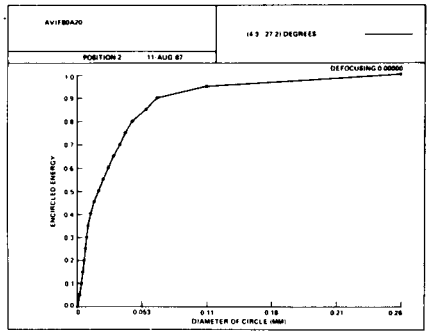

(2A) 550.0 nm

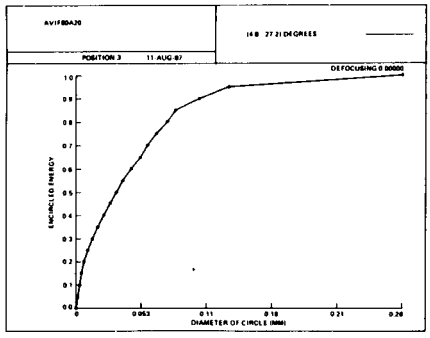

(3A) 440.0 nm

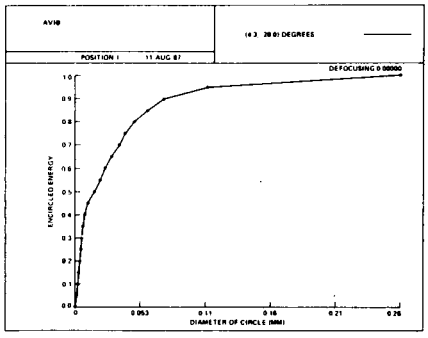

(1B) 1250.0 nm

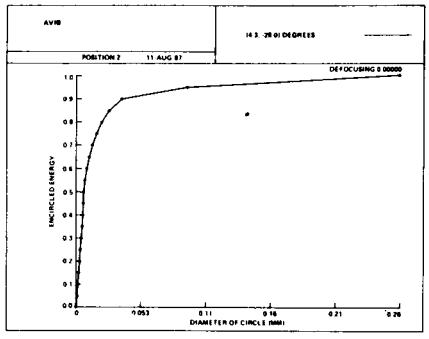

(2B) 950.0 nm

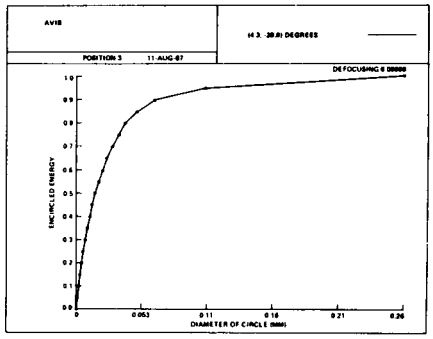

(3B) 650.0 nm

Fig. 6. Radial Energy Distribution

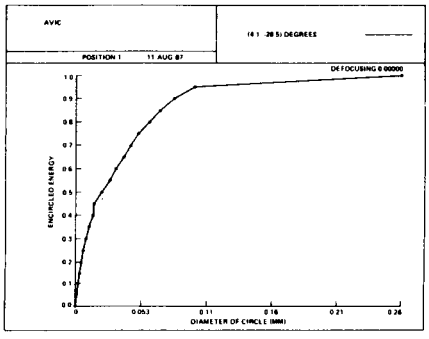

(1C) 1820.0 nm

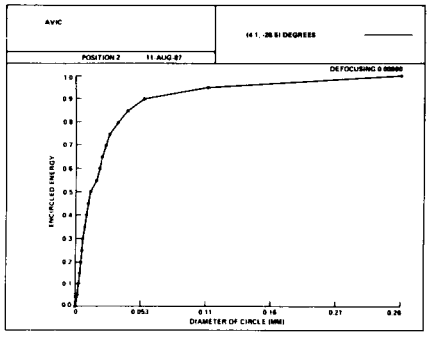

(2C) 1510.0 nm

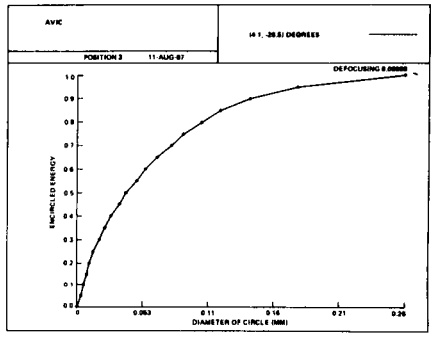

(3C) 1200.0 nm

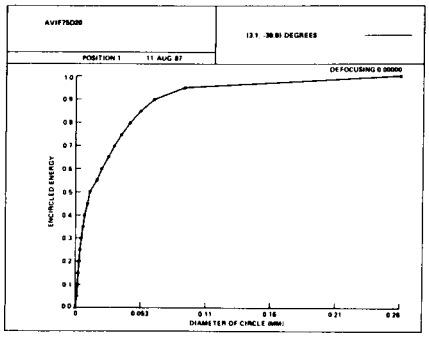

(1D) 2400.0 nm

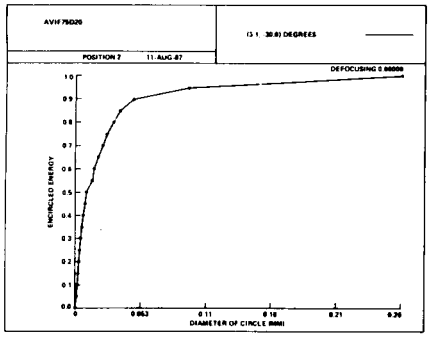

(2D) 2090.0 nm

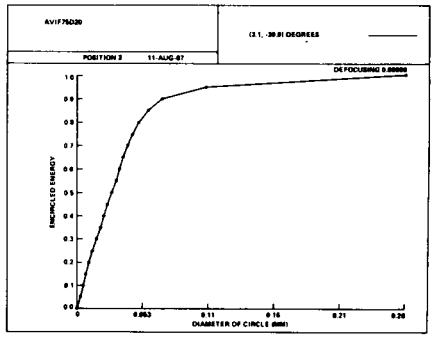

(3D) 1780.0 nm

Fig. 7. Radial Energy Distribution (Continued)

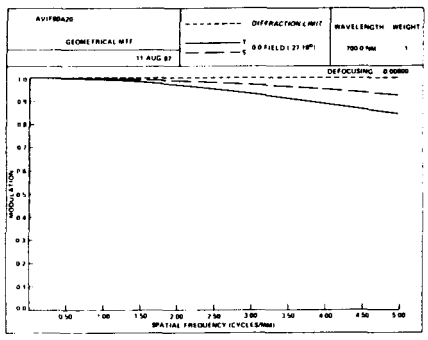

(1A) 700.0 nm

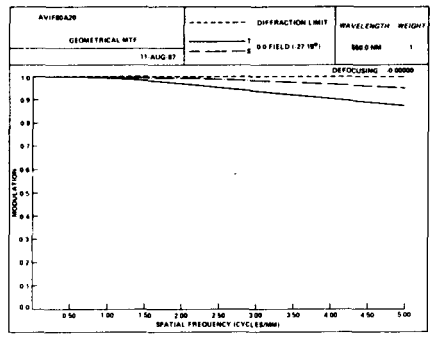

(2A) 550.0 nm

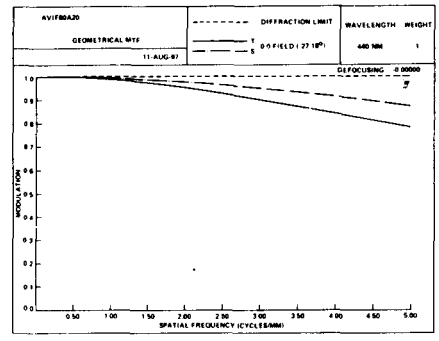

(3A) 440.0 nm

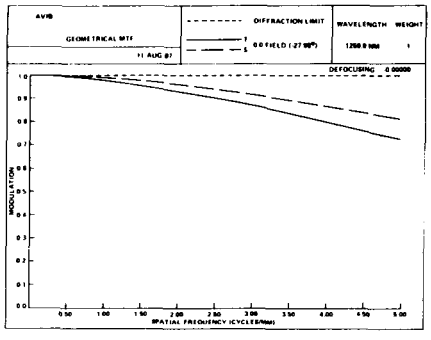

(1B) 1250.0 nm

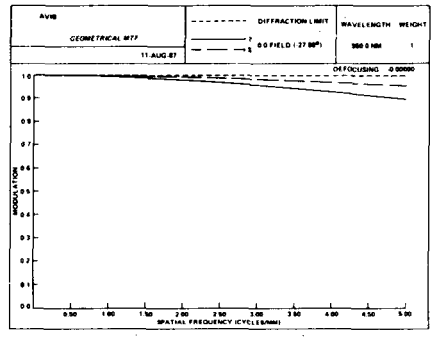

(2B) 950.0 nm

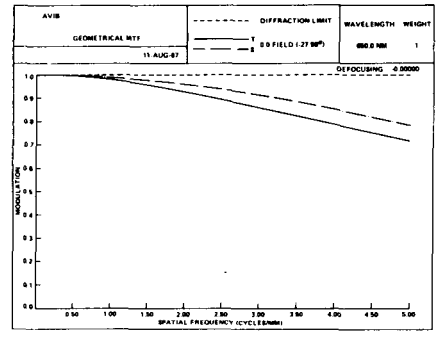

(3B) 650.0 nm

Fig. 8. AVIRIS Geometrical MTF

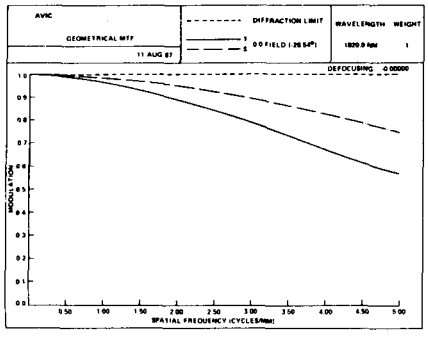

(1C) 1820.0 nm

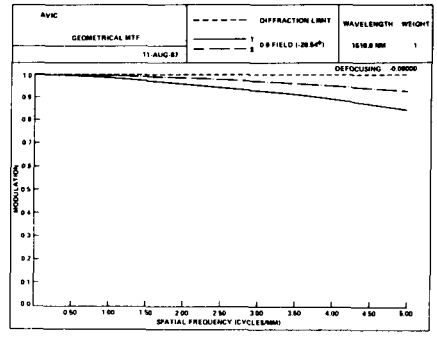

(2C) 1510.0 nm

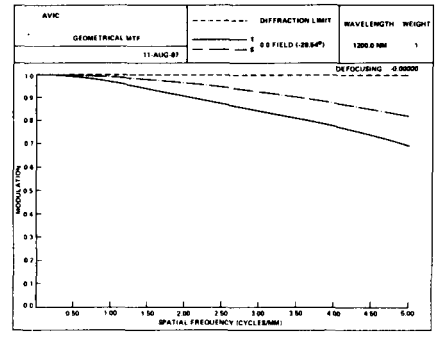

(3C) 1200.0 nm

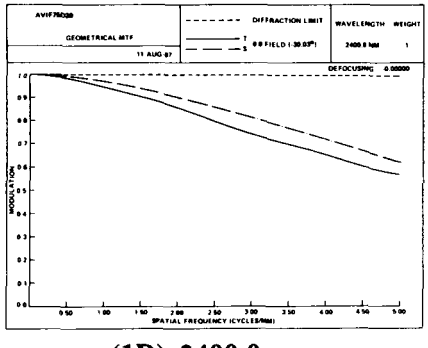

(1D) 2400.0 nm

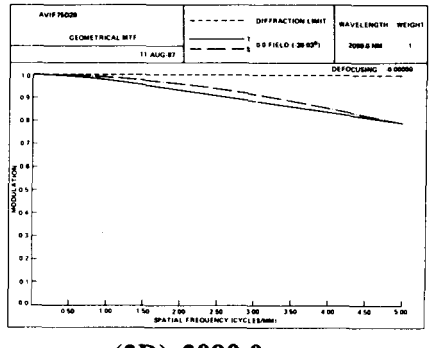

(2D) 2090.0 nm

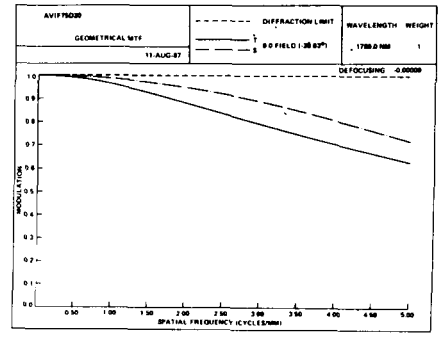

(3D) 1780.0 nm

Fig. 9. AVIRIS Geometrical MTF (Continued)

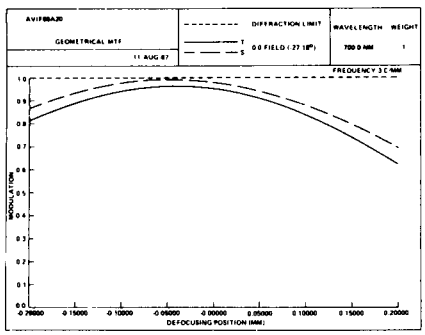

(1A) 700.0 nm

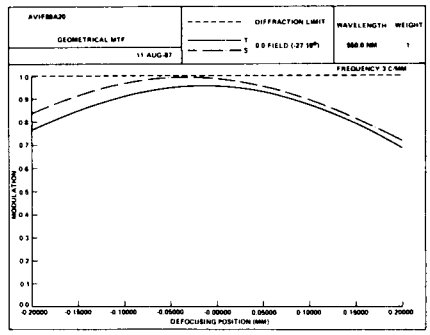

(2A) 550.0 nm

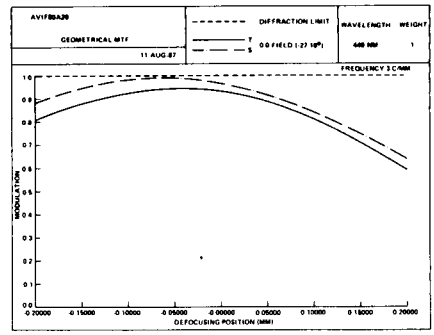

(3A) 440.0 nm

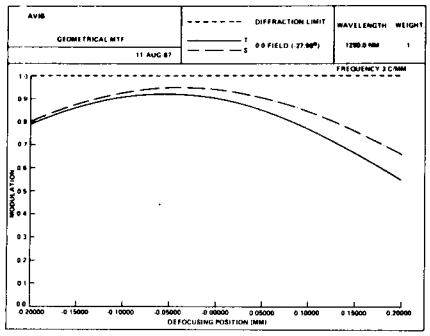

(1B) 1250.0 nm

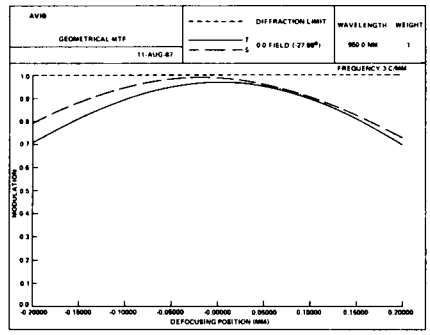

(2B) 950.0 nm

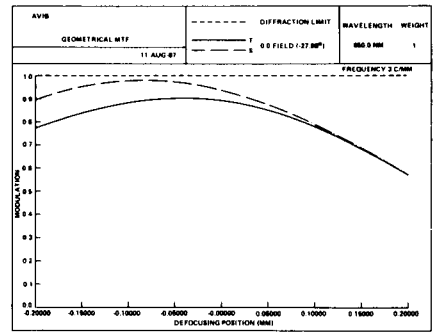

(3B) 650.0 nm

Fig. 10. AVIRIS Through Focus MTF

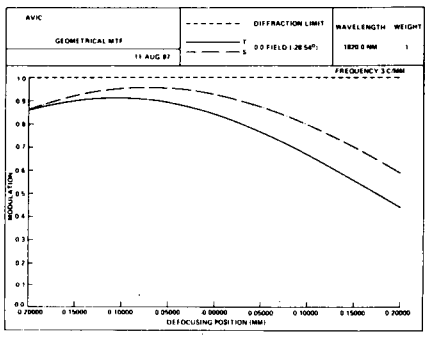

(1C) 1820.0 nm

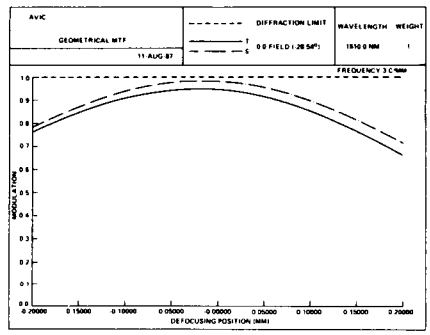

(2C) 1510.0 nm

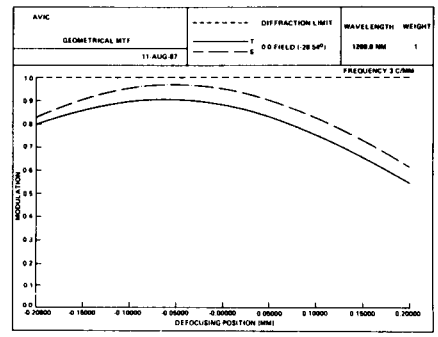

(3C) 1200.0 nm

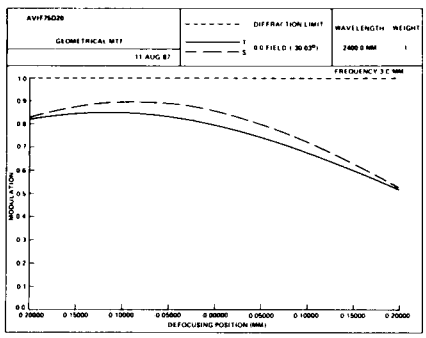

(1D) 2400.0 nm

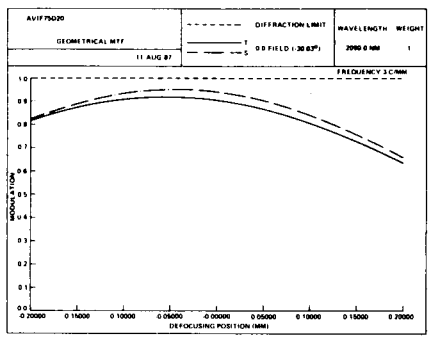

(2D) 2090.0 nm

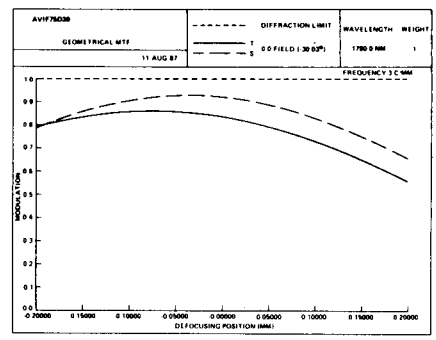

(3D) 1780.0 nm

Fig. 11. AVIRIS Through Focus MTF (Continued)

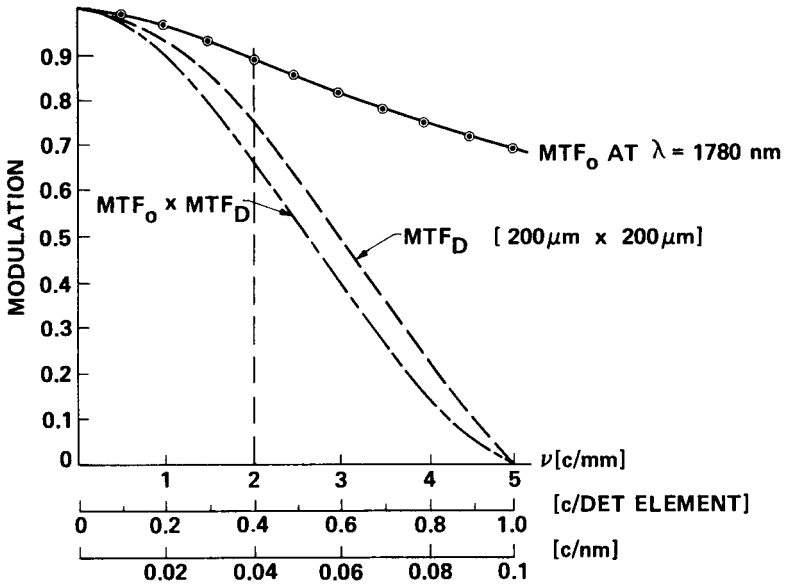

Fig. 12. AVIRIS System Modulation Transfer Function

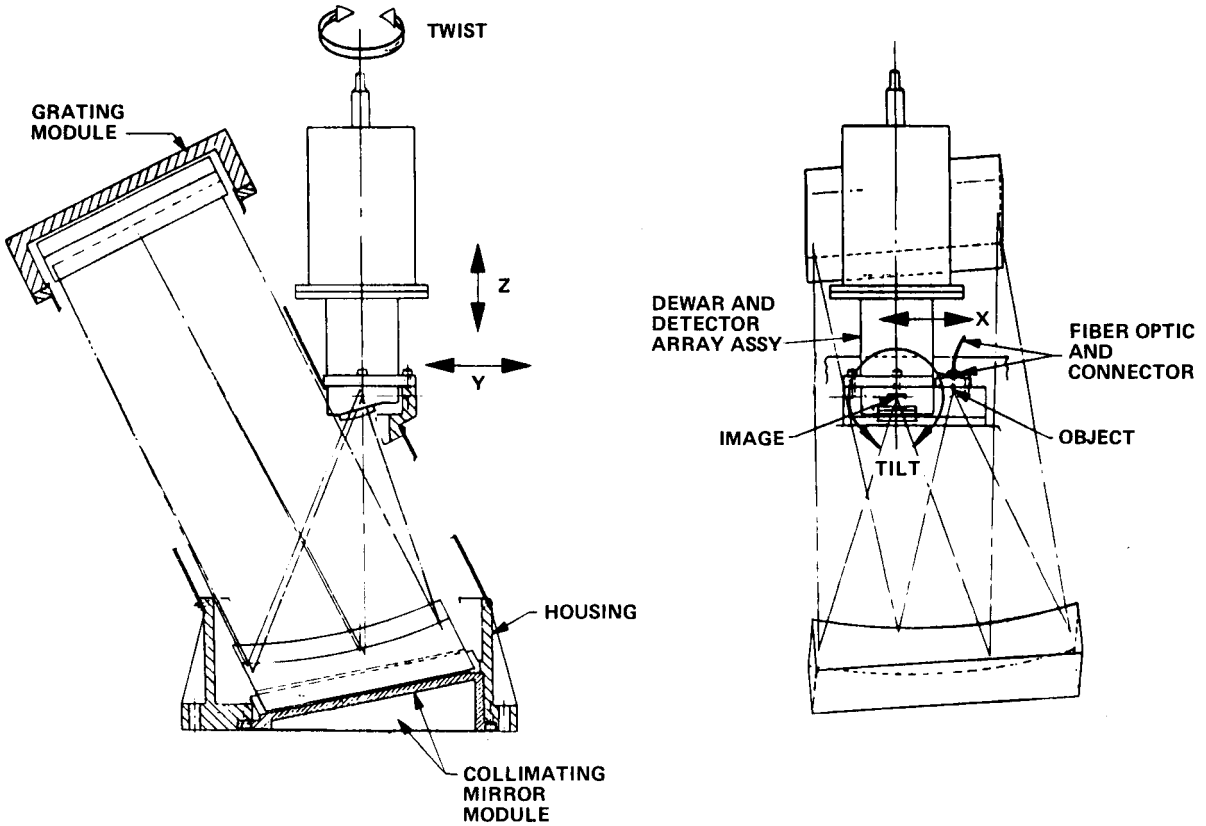

Fig. 13. AVIRIS Spectrometer Schematic

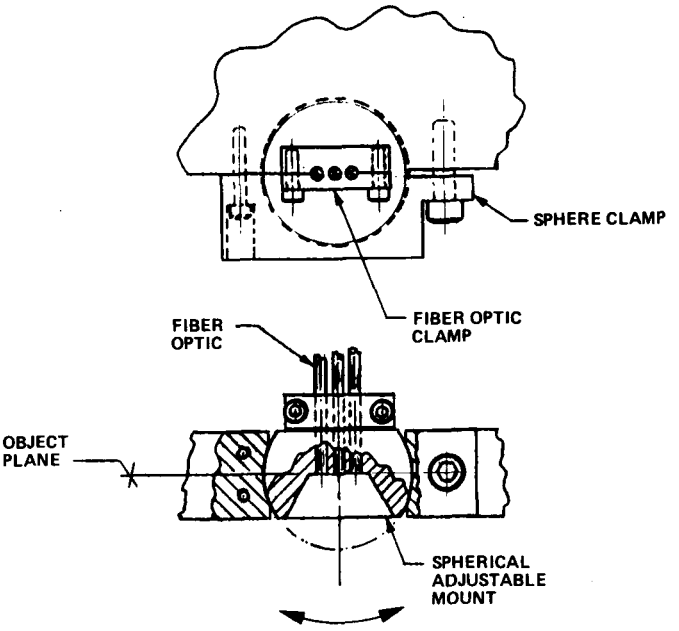

Fig. 14. AVIRIS Fiber Optics Mount

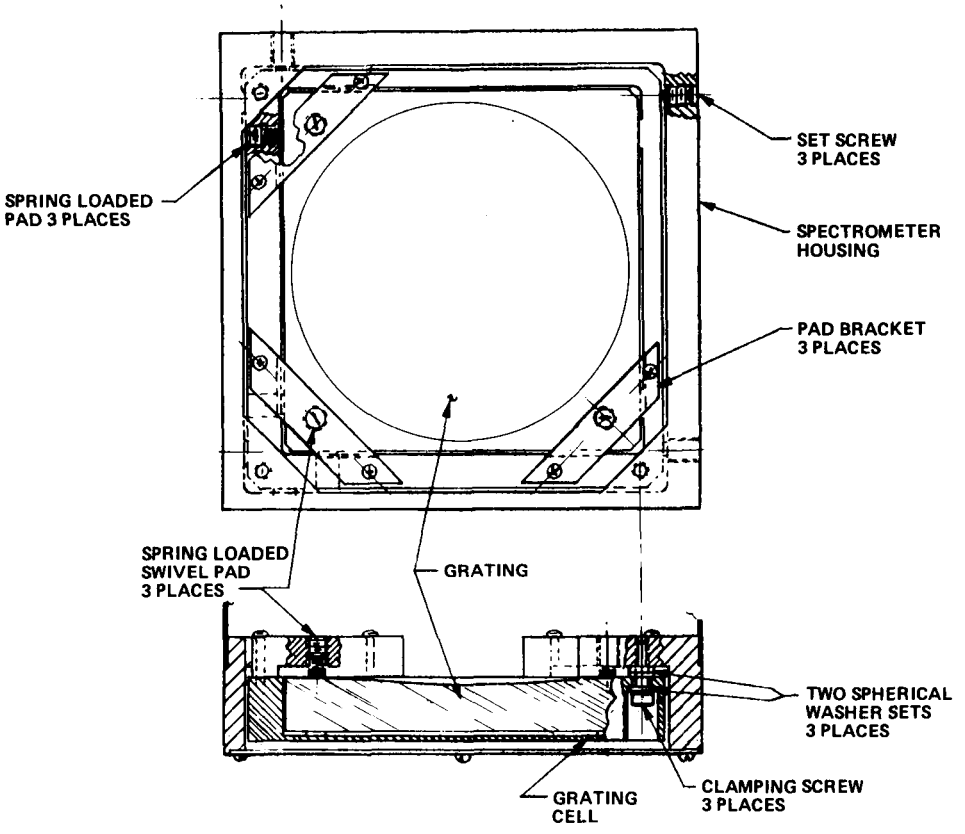

Fig. 15. AVIRIS Grating Mount

4. CONCLUSIONS

Tests of the fabricated spectrometers show that their image quality is sufficient to meet the required design goal of an MTF >0.5 at a spatial frequency of 2.0 c/mm for the spectrometer systems. Since completion of the system integration and radiometric calibration, AVIRIS has completed several test flights. The spectral images of the selected test sites, given in the accompanying papers in this session, are the best indication of the system performance under actual operating conditions.

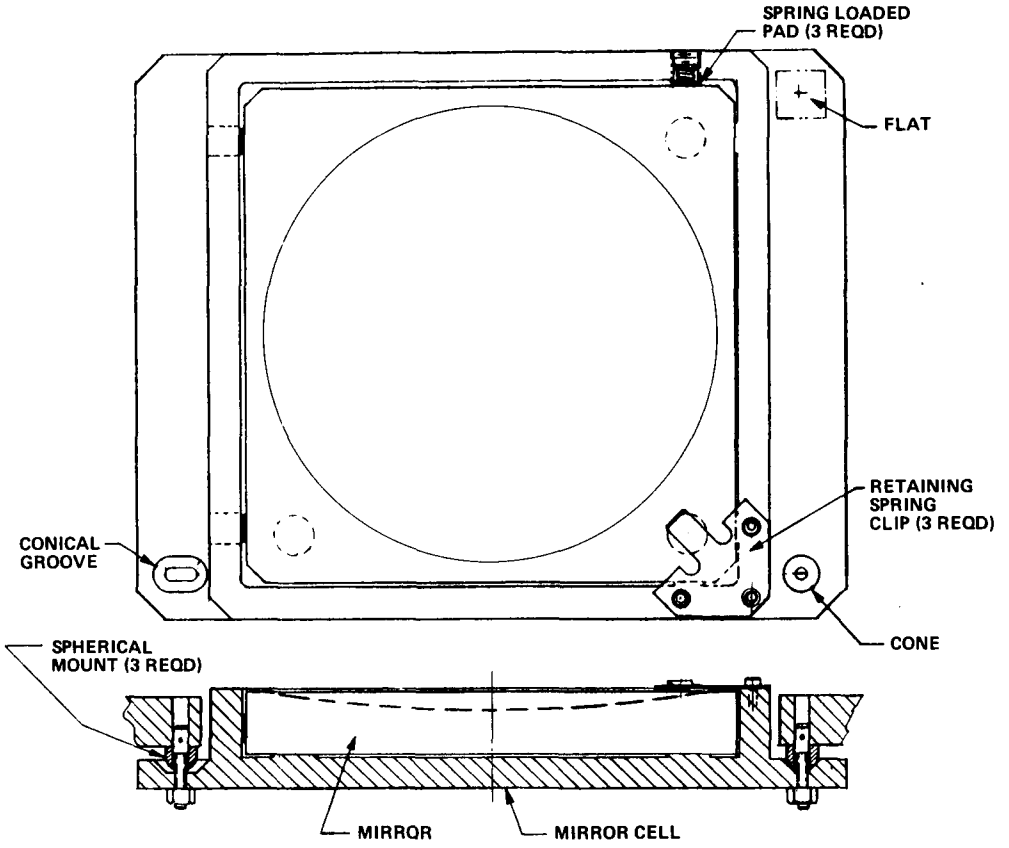

Fig. 16. AVIRIS Mirror Mount (Kinematic)

ACKNOWLEDGEMENTS

We would like to express our thanks to all members of the AVIRIS Design and Development Team for their support. The work described in this paper was supported by the Jet Propulsion Laboratory, California Institute of Technology, under a contract with the National Aeronautics and Space Administration.

REFERENCES

1. M. Herring, J. E. Duval and S. A. Macenka, "Development of the imaging spectrometer: technical challenges and solutions," SPIE 109-15.

2. M. Herring, G. C. Bailey, P. N. Kupferman, and S. A. Macenka, "Astronomical camera using a high-performance indium antimonide linear array," SPIE 501-38.

3. G. Vane, M. Chrisp, H. Enmark, S. Macenka and J. Solomon, "Airborne visible/infrared imaging spectrometer (AVIRIS): an advanced tool for earth remote sensing," Proc. 1984 IEEE Geoscience and Remote Sensing Symp., European Space Agency, SP215, Vol. 2, 1984.

4. C. LaBaw, "Airborne Imaging Spectrometer: an advanced concept instrument," SPIE 430-10.

5. M. P. Chrisp, J. B. Breckinridge, S. A. Macenka, and N. A. Page, "Imaging spectrometers for remote sensing from space," SPIE Vol. 589, 1985.

6. S. A. Macenka, "Near-infrared mapping spectrometer optical subsystem development and testing," SPIE 430-36.

7. P. N. Slater, Remote Sensing, Optics and Optical Systems, pp. 517-522, Addison-Wesley, 1980.

8. P. N. Slater, "Use of MTF in the specification and first-order design of electro-optical and photographic imaging and radiometric systems," Optica Acta, Vol. 22, No. 4, pp. 277-290 (1975).